ADAPTIVE NULLSTEERING OF MAIN LOBE JAMMING; ANALYSIS OF THE ARTIST TRIALS

A. Theil

TNO Physics and Electronics Laboratory
P.O. Box 96864
2509 JG The Hague
Netherlands

ABSTRACT

This paper considers the effectiveness of adaptive nullsteering in main lobe jamming scenarios. Four variants of algorithms are evaluated using data that has been gathered experimentally with an eight element array radar operating at C-band. The measurements were conducted in a coastal environment. Compared to fixed beamforming, an improved detection capability is clearly demonstrated. Furthermore, clutter suppression prior to weighting yields further improvements under adverse weather and sea state conditions.

Keywords: Adaptive Nullsteering, Mainlobe Jamming

1. INTRODUCTION

Main lobe jamming arises when the angular separation between a target and a jammer is less than the main lobe's width. In that case, the detection performance of a radar will be significantly degraded. For radars that are provided with multiple receive antennas and receiver channels, adaptive nullsteering can be employed to remedy the situation. This technique adapts the sensitivity pattern of the sensor array to the environment by steering 'nulls' in the directions of interfering sources. Knowledge about the number of jammers and their directions of arrival is not required. Jammers that transmit during a substantial part of the dwell can be cancelled; adaptive nulling is not effective against jammers that imitate the radar waveform.
The impact of adaptive nullsteering in main lobe jamming scenarios has been investigated in the Dutch research programme ARTIST (*Advanced Radar Techniques for Improved Surveillance and Tracking*). This paper presents the analysis of data that has been gathered during the ARTIST trials. The effectiveness of several variants of adaptive nulling algorithms is discussed. In particular, the effects of clutter are described.
The paper is organized as follows: The general setup of the experiments and the equipment is discussed in Section 2. Subsequently, details of adaptive nulling algorithms that have been employed are discussed. Results are presented in Section 4 where two representative measurements conducted under different weather conditions are discussed. Conclusions are formulated in Section 5.

2. EXPERIMENTAL SETUP AND EQUIPMENT

The setup for the main lobe nulling experiments as employed during the ARTIST trials is shown schematically in Figure 1. The jammer was positioned at a distance of 160 m from the radar. A helicopter flew radial trajectories over sea at a constant altitude and speed at the same azimuth as the azimuth of the jammer. As the target approaches, the angular separation between the target and the jammer elevation increases causing (elevation) main lobe jamming to transit to side lobe jamming. This transition is obtained when the target elevation varies at least 5.5° (half the aperture's 3 dB beamwidth in elevation) during the run. Typically, a target altitude of 500 m, a radar antenna altitude of 20 m and a jammer elevation of 2.0° was employed, while the helicopter travelled at a speed of 60 m/s between ranges of 2 and 12 km. This results in target elevations of 13.5° and 2.3° respectively (4/3 earth radius). Note that, viewed from the radar, the jammer is in front of the target.
The jammer transmitted a noisy waveform continuously in time within a band that covers the radar's frequency band. An experimental C-band surveillance radar with eight antenna elements stacked on top of each other, provided input data. The rotation rate is 27 RPM. The radar transmissions are burst oriented. The carrier frequency and Pulse Repetition Frequency (PRF) change from burst to burst. Polarization is horizontal.
Owing to a limited maximum data rate of the recording device, only data within a window bounded in range and azimuth was stored.

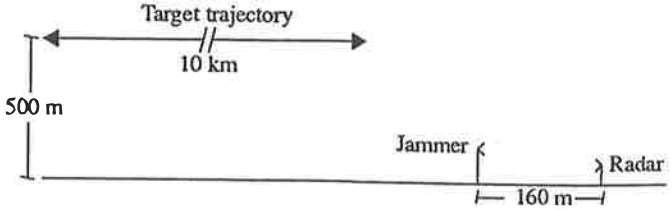

Figure 1 Configuration of main lobe nulling experiment depicted schematically (side view).

3. Theoretical Aspects

Since the principle of adaptive nullsteering can be found in numerous textbooks (Monzingo and Miller [1], Hudson [2]), this Section gives only a concise description. The combining network as depicted in Figure 2 is considered. The outputs of N sensors are weighted and subsequently summed producing an output signal y. The values of the weights determine the shape of the array beam pattern.

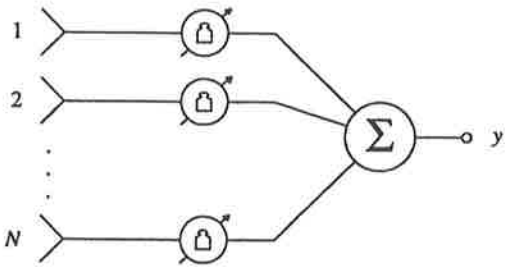

Figure 2 General scheme of a combining network.

An observation vector $\underline{z}$ is an N-dimensional vector containing the sensor outputs, each measured at the same point in time. The complex weighting vector is denoted as $\underline{w}$. The output signal of the network is given by

$$y = \underline{w} \cdot \underline{z} \tag{1}$$

A steering vector is defined as the vector that describes the relative phase at each sensor of a wave front arising from a far field source. To define a steering vector, knowledge of the positions of the sensor elements is required. If no interfering sources are present one may employ a weight vector that compensates the mutual phase differences of the signals received from a desired direction of arrival (DOA). The main beam of the pattern will then point in the desired direction and the elements of the weight vector are the complex conjugates of the corresponding elements of a steering vector $\underline{d}$ in the DOA:

$$\underline{w}_q = \underline{d}^* \tag{2}$$

The asterisk denotes the complex conjugate operation. In the presence of interference sources it may be favourable to employ a different set of weights in order to improve the suppression of these signals. The following criterion can be used to find optimum weights: Minimize the output power subject to the constraint that the gain in the desired DOA is held at a constant value. The constraint is introduced to prevent that the filter adapts to the nullvector. This constraint minimization problem can be solved using the method of Lagrange multipliers. The solution is given by the so-called Wiener-Hopf equation, [1]:

$$\underline{w}_{opt} = \mu \underline{M}^{-1} \underline{d} \tag{3}$$

$\underline{M}$ is the interference plus noise covariance matrix, μ is a scalar constant.
One should note the remarkable simplicity of the Wiener-Hopf equation. Weight calculation is an open loop procedure; there is no feedback from the filter output. Furthermore, *a priori* knowledge concerning the number of interfering sources and their locations is not required. The number of signals that can be nulled is limited to N - 1. In radar applications, the covariance matrix is not a priori available. The matrix must therefore be estimated from the received data. Suppose that K observation vectors $\underline{z}_k$ are available. $\underline{M}$ can be estimated by averaging over these

observation vectors according to:

$$\hat{\underline{M}} = \frac{1}{K}\sum_{k=1}^{K} \underline{x}_k \underline{x}_k^H \tag{4}$$

suffix 'H' denoting Hermitian transpose. Once a weighting vector is obtained, the output of the nullsteering filter corresponding with data vector $\underline{z}_k$, y, is calculated according to

$$y = \underline{w}_{opt} \cdot \underline{z}_k \tag{5}$$

3.1 Clutter Suppression

Since the nullsteering filter can cope with only a limited number of interfering sources, the presence of clutter can degrade its performance, see Theil [3]. One would therefore like to prevent that 'cluttered' observation vectors are taken into account in the formation of the covariance matrix. There are several ways to achieve this:

1. Selection of observation vectors with low clutter content. This option rules out the use of high PRFs.
2. Clutter removal prior to adaptive nullsteering. This requires that clutter suppression filters must be implemented in each sensor channel.
3. Gathering observation vectors while (temporarily) operating in a passive mode.

The first two options and their combination have been investigated in this research. For option 1 we use 16 (sweeps) × 50 (range quants) observation vectors from a distant range interval between 10 and 14 km from the radar. With respect to the algorithm, this implies that the range quant summation in equation (4) is modified. For option 2 we employ a middle velocity filter (MVF) to obtain clutter free observation vectors. The MVF is in essence a FIR filter whereby datavectors are integrated according to a Doppler shift that is half the blind speed. This operation does reduce the number of observation vectors.

3.1 Multiple Beams on Receive

To obtain adequate elevation coverage, six simultaneous beams stacked in elevation are employed. Each beam requires its own weight vector which is calculated according to equation (3). The inverted covariance matrix need, however, only be calculated once.

The principle of adaptive nullsteering for beams that are stacked in elevation is illustrated in Figure 3. The left diagram shows the patterns of six quiescent beams. The effect of adaptive nulling is depicted at the right where the beams adapt to a jammer situated under an elevation of 10°. Note that especially the shape of the one but lowest beam is altered significantly. This particular beam is indicated by a dashed line.

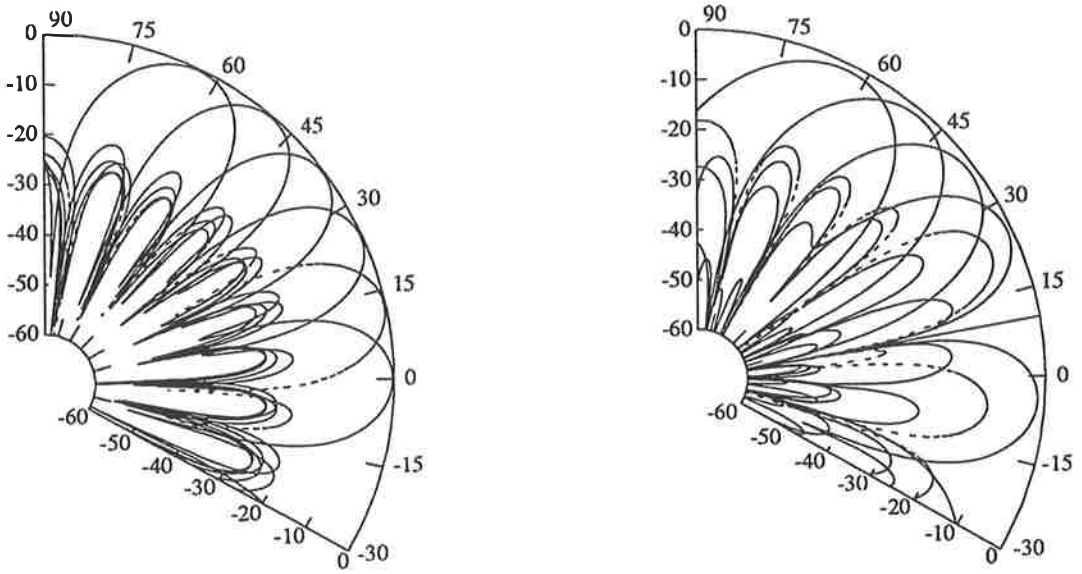

Figure 3 Six quiescent beams stacked in elevation (left) and six adaptive beams (right). The jammer elevation is 10°.

4. RESULTS

In this Section, results are discussed of two outbound runs of which the geometrical parameters have been described in Section 2. During the first run, sea state and wind force were relatively low. The second run, however, was conducted during a hail storm. The wind force was 7 Beaufort an the sea state was 5. For both runs a Jammer to Noise Ratio of 23 dB was employed.
To be able to demonstrate the effect of adaptive nullsteering, results without nullsteering are presented as well. In this case the weight vectors are calculated according to equation (2). Besides the options 1 and 2 and their combination to reduce the influence of clutter on the determination of the covariance matrix $\underline{M}$, results are also presented for the case that no anti-clutter measure is taken.
The diagrams presented in this Section show the estimated range and radial velocity of radar plots that emerge from the recording window. A negative velocity corresponds to an outbound target. Prior to the plot extraction process, the following operations are performed: digital beam forming, Doppler filtering in six beams, detection in six beams and in each Doppler bin per beam, and clustering in elevation, range and in azimuth.

4.1 First Run

Data were recorded during 80 scans. The size of the recording window was 7.0° by 11.6 km.
Figure 4 presents results when adaptive nullsteering is not activated. During the first 40 s of the run, the helicopter trail can easily be identified in both diagrams. From that point on, (incorrect) target speed estimates of approximately 50 m/s are often produced rather than -60 m/s. Since the radar operates in a velocity ambiguous mode, this indicates that the target is detected in only one burst. After 55 s the detection capability is degraded. Twenty scans do not produce any plots at all. The plots with a speed of approximately -15 m/s are caused by birds, flying downwind.

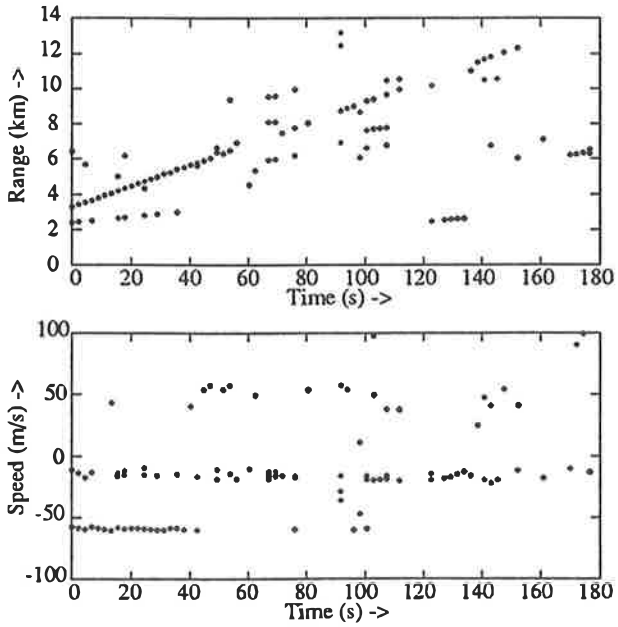

Figure 4 Estimated range (top) and velocity (bottom) versus time. Fixed beam forming is

It has been observed that in case jamming is not employed, the radar has no difficulty in producing target plots with correctly estimated range and velocity for this trajectory. The principle reason for the deteriorated detection capability (and hence the ability to solve the target velocity unambiguously) is the increased detection thresholds due to jamming. As a result, the target echo may go unnoticed which manifests itself beyond 6 km. We attribute the fact that the detection capability is regained at specific parts of the trajectory (for instance between 8 and 10 km) to the varying (azimuthal) alignment with the jammer during the course of the run.
Numerical information for the five different processing schemes is summarized in Table 1. The abbreviations and quantities used in this table denote the following:

- BF : Beamforming technique, either fixed or adaptive nulling (AN).
- CS : Clutter Suppression technique, see Section 3.

- N_{tot} : The total number of plots generated within the recording window.
- N_r : The number of target plots with correct range estimate.
- N_v : The number of target plots with correct speed estimate.
- S_{pl} : The number of scans without plots.
- P_r : The number of target plots per scan, given by:

$$P_r = \frac{N_r}{S} \tag{6}$$

with S the number of processed scans.

- $P_{r,nt}$: The number of non-target plots per scan. This quantity is calculated according to:

$$P_{r,nt} = \frac{N_{tot} - N_r}{S} \tag{7}$$

Table 1 Numerical information of the first run.

BF	CS	N_{tot}	N_r	N_v	S_{pl}	P_r	$P_{r,nt}$
fixed	n.a.	104	40	22	20	0.50	0.80
AN	None	166	71	61	3	0.89	1.19
	1	155	73	63	2	0.91	1.03
	2	156	68	43	3	0.85	1.10
	1 & 2	157	71	52	2	0.89	1.08

Adaptive nulling combined with the selection of distant observation vectors (option 1) provides best results with respect to both the number of target plots and the number of non-target plots. The benefit of the selection mechanism is, however, not significant. Figure 6 presents the results obtained with this particular processing scheme. Note that target plots with correctly estimated range and velocity are now produced up to a range of 12 km. The angular separation with the jammer at that point is less than 1/10th of the 3 dB beam width. For the lowest beam, a Jammer Cancellation Ratio (JCR) of 41 dB is achieved.

An increase in the number of non-target plots (birds, clutter and noise) can be noted as side effect of adaptive nulling. This phenomenon is caused by the increased side lobe level of the adaptive beams. For the favoured technique the increase is 29%.

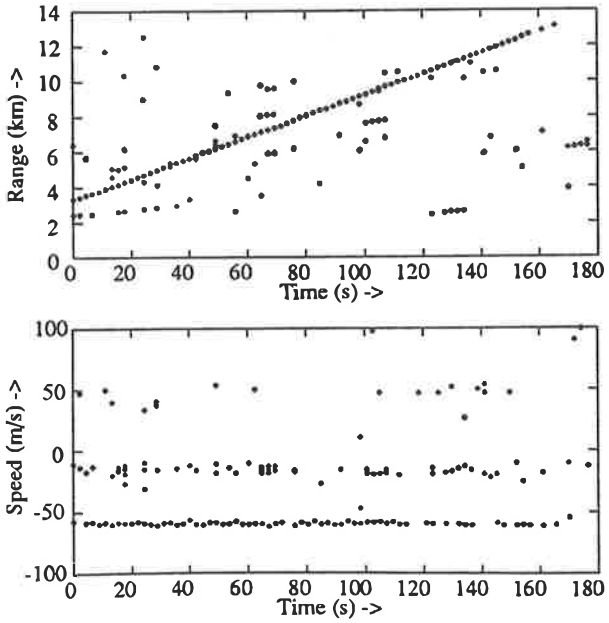

Figure 5 Results of first run obtained with adaptive nullsteering using selected observation vectors for weight calculation (option 1).

4.2 Second Run

During the second run, recordings were made during 112 scans using a recording window with size 12.6° by 10.4 km. The velocity of the helicopter was approximately 40 m/s.
Figure 7 presents results obtained with fixed beamforming. Beyond a range of 6 km only four target plots were produced which indicates that a better alignment with the jammer was achieved than during the first run. Numerical information is presented in Table 2.

Table 2 Numerical information of the second run.

BF	CS	N_{tot}	N_r	N_v	S_{pl}	P_r	$P_{r,nl}$
fixed	n.a.	114	42	40	37	0.38	0.64
AN	None	499	84	74	1	0.75	3.71
	1	378	86	74	2	0.77	2.61
	2	447	92	83	0	0.82	3.17
	1 & 2	403	94	85	0	0.84	2.76

Note that the techniques that employ the MVF produce most target plots while the use of distant data vectors brings about a significant reduction of the number of non-target plots. Due to the heavy clutter conditions the increase of the number of non-target plots is much higher than during the first run.
Figure 8 presents results obtained with adaptive nulling using selected observation vectors that are middle velocity filtered before calculation of the weights.

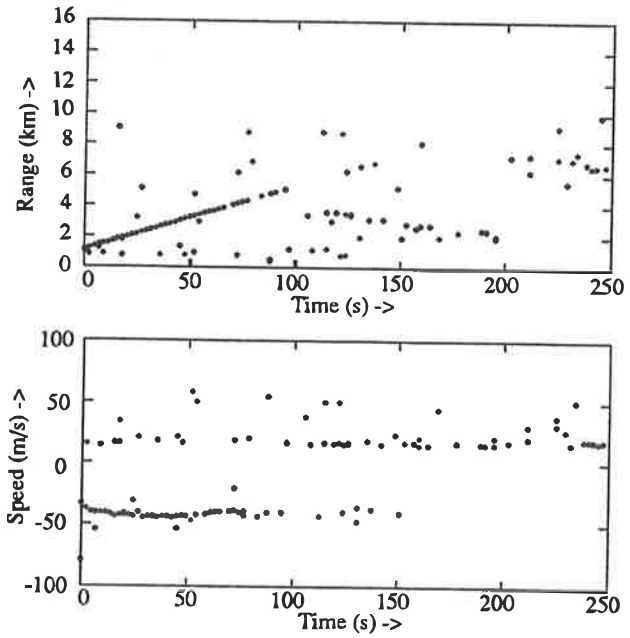

Figure 6 Results of the second run; fixed beam forming is employed.

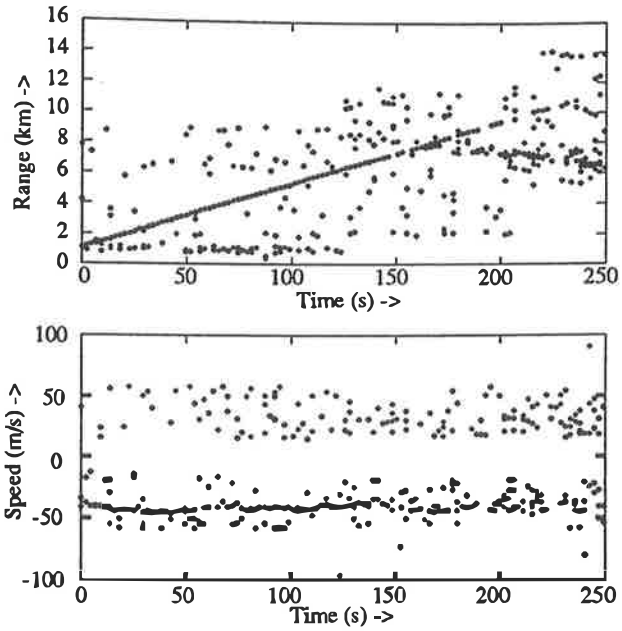

Figure 7 Results of second run; adaptive nullsteering using options 1 and 2.

5. CONCLUSIONS

The results presented in this paper support the effectiveness of adaptive nullsteering in main lobe jamming scenarios. Compared to fixed beam forming, the technique provides an improved detection capability which is expressed in a higher number of target plots and in an enhanced quality of estimated target parameters. An increased number of non-target plots has been observed as side-effect of adaptive nullsteering, especially under adverse weather and sea state conditions.
With respect to the optimal algorithm, clutter suppression prior to weighting is to be preferred.

6. REFERENCES

[1] R.A. Monzingo, T.W. Miller, *Introduction to Adaptive Arrays*, John Wiley and Sons, 1980, ISBN 0-471-05744-4.
[2] J.E. Hudson, *Adaptive Array Principles*, Peter Peregrinus Ltd., ISBN 0-906048-55-9.
[3] A. Theil, "On Combining Adaptive NullSteering with High Resolution Angle Estimation Under Main Lobe Interference Conditions," *IEEE AES Magazine*, November 1990

7. ACKNOWLEDGEMENT

ARTIST is an initiative in which Hollandse Signaalapparaten (SIGNAAL) and TNO Physics and Electronics Laboratory (TNO-FEL) investigate a variety of techniques that can lead to an improved quality of the air picture. The program is funded by the Ministry of Economic Affairs, the Ministry of Defence and SIGNAAL.